Osteoblast-like Cell Response to Titanium Coated with Co-Immobilized Elastin-Like Polymers Containing Integrin-Binding and Statherin-Derived Biomimetic Peptides

A THESIS
SUBMITTED TO THE FACULTY OF THE GRADUATE SCHOOL
OF THE UNIVERSITY OF MINNESOTA
BY

Eric Martin Beckman

IN PARTIAL FULFILLMENT OF THE REQUIREMENTS
FOR THE DEGREE OF
MASTER OF SCIENCE

Conrado Aparicio

May 2012

ACKNOWLEDGEMENTS

I would like to gratefully recognize my advisor Dr. Conrado Aparicio for his encouragement and assistance in developing, executing, assessing, and writing this research project. Thank you for providing such a supportive environment that simultaneously promoted critical thinking and inspired me to develop my best work.

I would also like to recognize my committee members, including Dr. Conrado Aparicio, Dr. Larry Wolff, and Dr. James Hinrichs. Each motivated me to develop a more articulate and meaningful research project and paper.

Thank you to those who have been involved in the various stages of this project, including experiment execution, data collection and analysis. More specifically, I would like to thank Dr. Yuping Li, Jeevan Govindharajulu, and Xi Chen for guidance with disc preparations, cellular assays, and statistical analysis. I would also like to acknowledge Drs. Raj Gopalakrishnan and Eric Jensen for their advise as well as laboratory support. I would also like to recognize J. Carlos Rodriguez-Cabello for fabricating the elastin-like peptide-containing polymers, a critical component of my research.

I wish to acknowledge Dr. Mark Herzberg for his mentorship over the years. His guidance helped develop my research critical thinking skills.

I would also like to thank my in-laws, Shelley and Steve, for their encouragement as well as for stress-reducing weekends in Milwaukee.

I would like to thank my parents, Tom and Mary Margaret, for their constant encouragement in any direction I have taken. They inspired me to be a better person through example, and I feel privileged and lucky to have had such loving parents.

Lastly, I would like to thank my wife, Lauren, for her unconditional love and support. We went into our graduate school programs with apprehension, but I feel that we have risen to each challenge by complimenting each other's strengths.

ABSTRACT

Endosseous implants are important options for restoring edentulous dental sites. Patients and practitioners are interested in implant systems that can osseointegrate faster and predictably in compromised patients. Recent research has shown that utilizing biomimetic peptides (i.e. RGD and SNa15) on titanium surfaces could improve osteoblastic responses. RGD is a peptide sequence important in binding nearly half of all integrins and is important in cellular adhesion. SNa15 is a modified peptide sequence from the N-terminus of the salivary protein statherin, which has been shown to be important in calcium phosphate mineral binding and nucleation. The aim of this study was to compare the *in vitro* outcomes associated with osseointegration (osteoblast-like cell adhesion, spreading, proliferation, and differentiation) between the titanium surfaces coated with RGD, SNa15, or a combination of the two biomimetic peptides via a covalently bound elastin-like biopolymer (p-). The co-immobilized titanium surfaces had either a 1:1 molar ratio of biomimetic peptides on separate biopolymers (pRGD and pSNa15) or a coating containing both peptides on a single biopolymer (pRGD-SNa15). Cellular adhesion, spreading, and proliferation was assessed with fluorescent labeling of actin, vinculin, and/or nuclear DNA and viewed with a light microscope. ELISA was used to determine early- and late-stage osteoblastic differentiation by measuring alkaline phosphatase and osteocalcin, respectively. Our results indicate that while titanium surfaces coated with only pRGD displayed greater cell adhesion, there were non-significant differences between titanium surfaces coated with elastin-like peptide polymers in terms of other osseointegration-related outcomes. We also noted a pattern that titanium surfaces coated with hydrophobic RGD-containing polymers were associated with an abnormal late stage osteoblastic differentiation pattern. In conclusion, we suggest that the co-immobilization of these biomimetic peptides via elastin-like polymers should be optimized in further research to improve their clinical applicability.

TABLE OF CONTENTS

ACKNOWLEDGEMENTS ..... **i**

ABSTRACT ..... **ii**

LIST OF TABLES ..... **v**

LIST OF FIGURES ..... **vi**

LIST OF ABBREVIATIONS ..... **vii**

Osteoblast-Like Cell Response to Titanium Coated with Co-Immobilized Elastin-Like Polymers Containing Integrin-Binding and Statherin-Derived Biomimetic Peptides **1**

INTRODUCTION **2**

Hypotheses 7

MATERIALS AND METHODS **8**

Materials 8

Synthesis of Elastin-like Peptide-Containing Polymers (ELPPs) 8

Surface Modification 8

Diffuse Reflectance Infrared Fourier Transform Spectroscopy (DRIFTS) 9

Contact Angle 10

Cell Culture Preparation 11

Cell Counting 11

Adhesion, Shaping, and Spreading 12

Proliferation 15

Differentiation 16

Total Protein Assay 17

Osteocalcin 18

Statistical Evaluation 19

RESULTS **20**

Surface Characterization: DRIFTS 20

Surface Characterization: Contact Angle 21

Cellular Adherence: Adhesion 22

Shaping and Spreading 26
Cellular Proliferation 28
Osteoblastic Differentiation: Alkaline Phosphatase 29
Osteocalcin 31
DISCUSSION 33
Contact Angle 33
Cell Adhesion 35
Proliferation 37
Differentiation 38
RGD 40
SNa15 42
CONCLUSIONS 43
REFERENCES 46

LIST OF TABLES

TABLE 1: AMINO ACID SEQUENCES FOR BIOMIMETIC PEPTIDES 4
TABLE 2: STRUCTURAL DESCRIPTION OF THE DIFFERENT ELASTIN-LIKE PEPTIDE POLYMER-COATED TITANIUM SURFACE GROUPS 5
TABLE 3: CONVERSION BETWEEN PIXELS AND DISTANCE 15

LIST OF FIGURES

FIGURE 1: SCHEMATIC REPRESENTATION OF COATING TITANIUM SURFACES WITH ELASTIN-LIKE PEPTIDE POLYMERS 6
FIGURE 2: CONTACT ANGLE..... 11
FIGURE 3: DIAGRAM OF IMMUNOFLUORESCENT INCUBATION SYSTEM..... 14
FIGURE 4: DRIFTS 20
FIGURE 5: CONTACT ANGLE..... 22
FIGURE 6: ADHESION AT TWO HOURS..... 24
FIGURE 7: ADHESION AT FOUR HOURS 25
FIGURE 8: CELL SHAPING AND SPREADING AT TWO HOURS 27
FIGURE 9: CELL SHAPING AND SPREADING AT FOUR HOURS 28
FIGURE 10: PROLIFERATION..... 29
FIGURE 11: ALKALINE PHOSPHATASE ACTIVITY 30
FIGURE 12: OSTEOCALCIN LEVEL..... 32

LIST OF ABBREVIATIONS

ALP: Alkaline phosphatase
CPTES: Silane unit (3-chloropropyl triethoxysilane) used to covalently bind elastin-like polymers to titanium
DAPI: Fluorescent stain (4',6-diamidino-2-phenylindole) for nuclear DNA
DDDEE: Acidic amino acids sequence found in statherin-derived peptide
DIEA: Diisopropylethylamine
DMEM: Dulbecco's modified eagle medium
DRIFTS: Diffuse reflectance infrared Fourier transform spectroscopy
ECM: Extracellular matrix
ELP: Elastin-like polymer
ELPP: Elastin-like peptide-containing polymer
FBS: Fetal bovine serum
HAP: Hydroxyapatite
MC3T3-E1: Murine pre-osteoblastic cells
OCN: Osteocalcin
PBS: Phosphate buffered solution
PEG: Poly(ethylene glycol)
PFA: Paraformaldehyde solution
pRef: Reference elastin-like polymer not containing a biomimetic peptide
pRGD: Elastin-like polymer with integrin-binding peptide
pSNa15: Elastin-like polymer with statherin-derived peptide
RGD: Integrin-binding peptide
rhBMP-2: Recombinant human bone morphogenetic protein 2
SNa15: Statherin-derived peptide
Ti-clean: Cleaned titanium disc
Ti-etched: Cleaned titanium disc with alkali etching
Ti-pRef: Clean and alkali-etched titanium disc with a reference elastin-like polymer
Ti-pRGD: Clean and alkali-etched titanium disc with an elastin-like polymer containing an integrin-binding peptide
Ti-pRGD-SNa15: Clean and alkali-etched titanium disc with an elastin-like polymer containing both an integrin-binding peptide and a statherin-derived peptide
Ti-pSNa15: Clean and alkali-etched titanium disc with an elastin-like polymer containing a statherin-derived peptide
Ti-1:1 pRGD to pSNa15: Clean and alkali-etched titanium disc coated with a 1:1 molar ratio of elastin-like polymers containing an integrin-binding peptide or a statherin-derived peptide
TRITC: Orange fluorescent dye (tetramethylrhodamine) conjugated with phalloidin for fluorescent staining F-actin

Osteoblast-Like Cell Response to Titanium Coated with Co-Immobilized Elastin-Like Polymers Containing Integrin-Binding and Statherin-Derived Biomimetic Peptides*

*In preparation for submission

INTRODUCTION

Endosseous titanium dental implants are one option for restoring function to edentulous sites. Conventional time needed after implant placement before the implants can be restored and loaded is 2 months.[1] If loading is performed before adequate osseointegration has occurred, soft tissue encapsulation and subsequent implant failure can occur.[2] During the time between implant placement and loading, patients typically have esthetically or functionally inferior restorations. Therefore, accelerating the rate of osseointegration of implants would improve patients' quality of life. Implant surface properties are one factor that may influence and improve earlier loading protocols.[3,4] Commercially pure titanium is commonly used for dental implants because of its mechanical properties, corrosion resistance, and biocompatibility. Unfortunately, titanium is not bioactive and thus causes passive osseointegration. Thus, implant technology has focused upon either improving the surface topography (i.e. roughness) or coating the surface of the titanium with a bioactive substance to accelerate osseointegration.[5]

Osseointegration of dental implants is dependent upon a stable mineralized bone matrix, which is established mainly by osteoblastic cells. There have been 4 described techniques to promote osteoblastic activity at the implant surface including osteoblast recruitment, attachment, proliferation, and differentiation.[6] Previous research has evaluated naturally occurring biomolecules (i.e. rhBMP-2) being coated on titanium surfaces to induce the recruitment of osteoblasts.[7] Unfortunately, these naturally occurring molecules cannot be structurally modified or optimized as easily as synthetic biomolecules and are not covalently bound to the titanium surface.

Osteoblast attachment to the titanium surface is also an important component in establishing and maintaining osseointegration. When osteoblasts attach to extracellular matrix (ECM) proteins via trans-membrane proteins (i.e. Integrins), a signaling pathway influences cellular growth and differentiation.[6] RGD is an amino acid sequence containing Arg-Gly-Asp, which is important in cell adhesion (Table 1). RGD is found on blood, extracellular matrix (i.e. fibronectin, vitronectin), cell-surface proteins, and is a key component in the recognition site for nearly half of all integrins.[8,9] As a consequence, previous studies have shown surfaces coated with RGD sequences have displayed improved cellular adhesion[10,11] and proliferation[12] compared to control surfaces. As with healing in other tissues, proliferation of osteoblastic cells is vital in implant osseointegration.[6] Even if pre-osteoblastic cells are recruited, attached, and proliferate at the surface of the implant, osseointegration is dependent upon the mineralization of the bone matix for support. As a consequence, promoting differentiation of pre-osteoblasts to osteoblasts for forming a mineralized bone matrix is the final target to promote osseointegration.[6] SNa15 is an amino-acid sequence from the N-terminus of the statherin molecule, which was noted to be the sequence associated with hydroxyapatite (HAP) binding.[13,14] The SNa15 sequence differs from the original 15 amino acids at the N-terminus of Statherin because the phosphoserines are replaced with Aspartic acid (D) amino acids (Table 1). This change did not alter the binding affinity for these sequences to HAP. The acidic domains of the amino acids (DDDEE) in SNa15 and it's helical conformation are the main reasons for its high affinity for hydroxyapatite.[14,15] Previous results in our lab demonstrated trends in improved *in vitro* osteoblast differentiation with titanium surfaces coated with SNa15 compared to control

surfaces.[16] In conclusion, it is well accepted that biomaterials that benefit osseointegration are those inducing the greatest adherence (cell spreading), proliferation, and cell differentiation to the osteoblastic lineage.

Table 1: Amino Acid Sequences for Biomimetic Peptides

Biomimetic Peptide Groups	**Amino Acid Sequence**
IK-24 Reference polymer (Ref)	No peptide (only elastin-like polymers present)
Integrin-binding domains (RGD)	AVTGRGDSPASS
Statherin-derived peptide (SNa15)	DDDEEKFLRRIGRFG
Combined Integrin-binding domain (RGD) with Statherin-derived peptide (SNa15)	AVTGRGDSPASS-DDDEEKFLRRIGRFG

Table showing the associated amino acid sequence of each biomimetic peptide. A: Alanine; D: Aspartic Acid; E: Glutamic Acid; F: Phenylalanine; G: Glycine; I: Isoleucine; K: Lysine; P: Proline; R: Arginine; S: Serine; T: Threonine; V: Valine.

Previous research[17] has already demonstrated that titanium surfaces can be covalently-coated with RGD and SNa15 by means of an elastin-like recombinant polymer (p-) via a silane unit (CPTES) (Table 2, Figure 1). A common elastin-like polymer (ELP) is composed of repeating pentapeptides of amino acid sequences of L-Valine[1]-L-Proline[2]-L-Glycine[3]- X[4]-L-Glycine[5] (VPGXG), where "X" is any natural amino acid except Proline.[18] ELPs are extracellular matrix (ECM) analogues that have been shown to act as vehicles for bioactive peptides.[19,20] ELPs are considered an appropriate vehicle because they are biocompatible[21] and can withstand mechanical forces similar to natural elastin.[22] Thus, we are utilizing ELPs to attach the bioactive peptides in order to create a biocompatible, mechanically stable, covalently bound bioactive coating to improve cellular response.

Table 2: Structural Description of the Different Elastin-Like Peptide Polymer-Coated Titanium Surface Groups

Titanium surface groups	**Titanium with bound Elastin-like Peptide Polymer Structure**
Ti-pRef	Ti-CPTES-[((VPGIG)$_2$-(VPGKG)-(VPGIG)$_2$)$_2$] - [((VPGIG)$_2$-(VPGKG)-(VPGIG)$_2$)$_2$]$_n$
Ti-pRGD	Ti-CPTES-[((VPGIG)$_2$-(VPGKG)-(VPGIG)$_2$)$_2$] - AVTGRGDSPASS - [((VPGIG)$_2$-(VPGKG)-(VPGIG)$_2$)$_2$]$_n$
Ti-pSNa15	Ti-CPTES-[((VPGIG)$_2$-(VPGKG)-(VPGIG)$_2$)$_2$] - DDDEEKFLRRIGRFG - [((VPGIG)$_2$-(VPGKG)-(VPGIG)$_2$)$_2$]$_n$
Ti-1:1 pRGD to pSNa15 (molar ratio)	TI-CPTES-[((VPGIG)$_2$-(VPGKG)-(VPGIG)$_2$)$_2$] - AVTGRGDSPASS - [((VPGIG)$_2$-(VPGKG)-(VPGIG)$_2$)$_2$]$_n$ And TI-CPTES-[((VPGIG)$_2$-(VPGKG)-(VPGIG)$_2$)$_2$] - DDDEEKFLRRIGRFG - [((VPGIG)$_2$-(VPGKG)-(VPGIG)$_2$)$_2$]$_n$
Ti-pRGD-SNa15	Ti-CPTES-[((VPGIG)$_2$-(VPGKG)-(VPGIG)$_2$)$_2$] – AVTGRGDSPASS-DDDEEKFLRRIGRFG - [((VPGIG)$_2$-(VPGKG)-(VPGIG)$_2$)$_2$]$_n$

Table displaying the amino acid structure of the polymer and bioactive peptide bound to titanium via a silane unit for each Elastin-like peptide-containing polymer (ELPP) coated titanium group. Black: Titanium (Ti) with silane unit (CPTES); Blue: Polymer amino acid sequence; Red: Biomimetic amino acid sequence; A: Alanine; D: Aspartic Acid; E: Glutamic Acid; F: Phenylalanine; G: Glycine; I: Isoleucine; K: Lysine; P: Proline; R: Arginine; S: Serine; T: Threonine; V: Valine.

Figure 1: Schematic Representation of Coating Titanium Surfaces with Elastin-Like Peptide-Containing Polymers

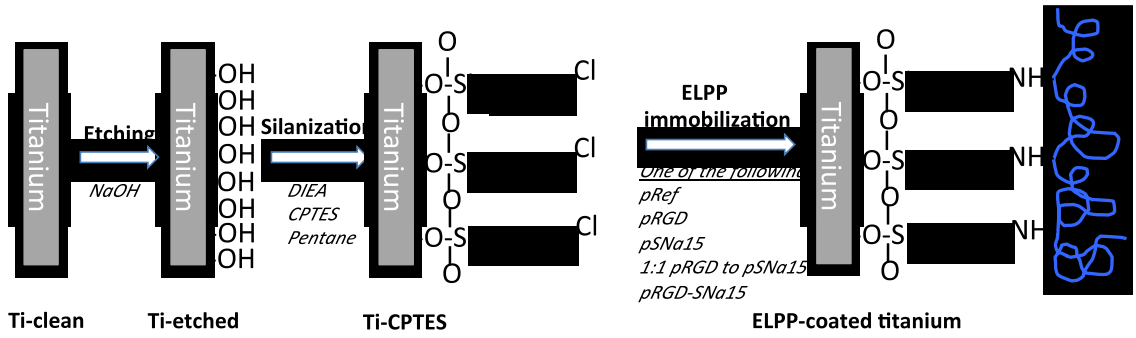

Schematic demonstrating the process to bind Elastin-like peptide-containing polymers (ELPPs) onto titanium. First, clean titanium is conditioned with alkali etching using NaOH to activate hydroxyl groups. Next the surface undergoes silanization to covalently bind CPTES. Finally, specific ELPPs are covelantly bound to the titanium via the silane unit to form the final ELPP-bound titanium surfaces.

Recently published research has also shown that titanium surfaces coated with pRGD and surfaces coated with pSNa15 improved the *in vitro* osteoblast response when compared to non-coated titanium surfaces and surfaces coated with ELPs without the functional peptides. Those surfaces with the RGD motif (Ti-pRGD or Ti-pRGD-SNa15) showed significantly greater adhered cell numbers after incubating 4 hours and subjectively greater adherence morphology than other titanium surfaces. Ti-pRGD-SNa15 surfaces also showed a trend of greater proliferation of osteoblasts as well as differentiation (alkaline phosphatase (ALP) and osteocalcin (OCN)) at the gene expression level compared to other titanium-modified surfaces.[16] One limitation of this previous research was that statistical assessments were not conducted to note statistical significance, and the differentiation was assessed at the expression level and not at the protein level.[16] Another gap in previous research is that a titanium surface coated a single molecule of two bioactive peptides (Ti-pRGD-SNa15) has not been compared with a

titanium surface coated with two molecules of bioactive peptides in a 1:1 molar ratio (Ti-1:1 pRGD to pSNa15).

Hypotheses

Based upon previous research and the preliminary results from our laboratory, we have constructed two main hypotheses. The first null hypothesis is that titanium surfaces coated with one elastin-like polymer carrying two bioactive peptides (Ti-pRGD-SNa15) will show no significant differences in pre-osteoblastic adhesion, spreading, proliferation and differentiation compared to titanium surfaces coated with an equal ratio of two separate elastin-like polymers, each carrying one of the two different peptides (Ti-1:1 pRGD to pSNa15). The second null hypothesis is that titanium surfaces coated with one bioactive peptide (Ti-pRGD or Ti-pSNa15) will demonstrate no significant differences in the same aforementioned cellular assays as the first hypothesis, when compared to titanium surfaces coated with two bioactive peptides (Ti-pRGD-SNa15 or Ti-1:1 pRGD to pSNa15) on the same surface.

We will compare titanium surfaces coated with different elastin-like peptide polymers (Ti-pRGD, Ti-pSNa15, Ti-pRGD-SNa15, and Ti-1:1 pRGD to pSNa15). Each experiment will test the bioactive response of pre-osteoblastic cells to the conditioned surface by qualifying the adherence and spreading of cells during attachment, as well as quantifying cellular proliferation and differentiation at the protein level.

MATERIALS AND METHODS

Materials

Surface modification and cell experiment reagents were purchased from Sigma-Aldrich (St. Louis, MO) unless otherwise specified.

Synthesis of Elastin-like Peptide-Containing Polymers (ELPPs)

Provided by Professor Carlos Rodriguez-Cabello from the University of Valladolid, Spain. Genetic engineering using standard methods as well as production of the elastin-like peptide polymers were conducted as described previously.[19,23,24] The elastin-like peptide polymers were engineered with 3 components: VPGIG, VPGKG (with the isoleucine replaced with a lysine to enable cross-linking), and one or two of the bioactive peptide sequences (Table 1) with a final structure as seen in Table 2.

Surface Modification

Commercially pure titanium (grade II) was obtained (10x10cm wide x 1mm thick titanium sheets) (McMaster-Carr, USA) and punched into 7.5mm diameter discs. One side of the disc was determined to be the conditioned side, while the other received an "X" to ensure it was placed down during disc conditioning. A schematic representation of surface modifications is illustrated in Figure 1. Discs were cleaned with cyclohexane for 10 minutes, then rinsed with distilled water and acetone and dried with nitrogen gas. Cleaned-titanium discs were then ready to use as a negative control group.

The discs were etched overnight in an alkali environment of 5M NaOH at 60°C, and cleaned with distilled water, acetone, and dried with nitrogen gas. Etched-titanium discs were then ready to use as a control group.

The discs were silanized in a reaction vessel in nitrogen gas environment with 3-chloropropyl triethoxysilane (CPTES), diisopropylethylamine (DIEA), and anhydrous pentane. The reaction had intermittent ultrasonic movement every 10 minutes for 2 minutes for a total of 60 minutes. After silanization, the discs were rinsed with ethanol, isopropanol, distilled water, acetone, and then dried with nitrogen gas. The discs were then coated with their respective biopolymer coating by immersion in a solution of 4.0mg biopolymer (pRGD, pSNa15, or pRGD-SNa15) in 8mL cold 0.5mg/mL Na_2CO_3 in a desiccator under argon atmosphere overnight. 1:1 pRGD to pSNa15 surface group had 1.4mg pSNa15 and 2.6mg pRGD in 8mL of Na_2CO_3 to establish a 1:1 molar-ratio of biopolymers. After biopolymer immobilization, the discs were rinsed with cold distilled water and acetone, air-dried, and stored in a paraffin-sealed and clean 48-well plate at 4°C.

The titanium discs then had surface characteristics measured with contact angle within 30 minutes of surface modification and DRIFTS.

Glass discs (10mm diameter coverslips, product#2603368, Ted Pella Inc., Redding, CA) were used as a positive control surface for cell experiments.

Diffuse Reflectance Infrared Fourier Transform Spectroscopy (DRIFTS)

Diffuse reflectance infrared Fourier transformed spectroscopy (i.e. DRIFTS) is an established technique for characterizing and identifying the proper coating of bioactive

polymers on titanium surfaces.[23,25] Surface modification of each titanium group was evaluated by diffuse reflectance infrared Fourier transform spectroscopy (Nicolet series II Magna-IR system 750) at a resolution of 4 cm^{-1} and scanning range from 650 cm^{-1} to 4000 cm^{-1}.

Contact Angle

Sessile drop contact angle measurements were obtained of each surface modified titanium disc group using a contact angle analyzer (DM-CE1, Kyowa Interface Science, Japan). A sequence of photos was taken from a lateral view of the titanium discs with a digital camera. The angle between the titanium disc surface and side of the droplet (Figure 2) was measured using an image analyzing software (FAMAS - Interface Measurement & Analysis System, Ver. 3.0.0, Kyowa Interface Science Co, LTD). Pictures were taken every second (1000 milliseconds) for 60 seconds starting immediately after a standardized droplet (1.5-2μL) of deionized water was placed on the disc. Three discs per surface group were measured and the mean contact angle was calculated. Comparisons were conducted between surface groups in terms of mean initial (0 seconds) and final (59 seconds) contact angles as well as the patterns in changing contact angle measurements over time.

Figure 2: Contact Angle

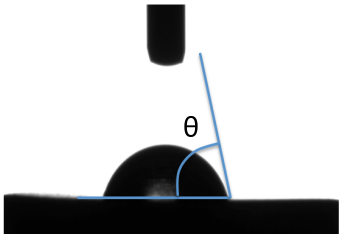

Figure displays the angle between the titanium surface and droplet edge at which contact angle was measured for each second for 60 seconds.

Cell Culture Preparation

Murine pre-osteoblastic MC3T3-E1 cells (ATCC, Manassas, VA) were cultured in Dulbecco's modified Eagle medium (DMEM) with 10% fetal bovine serum (FBS, Gemini Bio-Products, West Sacramento, CA) and 1% penicillin/streptomycin (Invitrogen, Grand Island, NY) at 37°C in an 5% CO_2 atmosphere with 100% humidity.

Cell Counting

Cells were counted before each assay. Cell dishes were removed from the incubator and the media was aspirated, followed by a rinse with HBSS. After aspirating the HBSS, Trypsin (1-2 mL) was added to the culture dish and incubated for 5 minutes at 37°C until cells were detached and rounded in appearance. Alpha-MEM (Invitrogen, Grand Island, NY) (7-8 mL) was added to the culture dish and transferred with the cells to a 15mL centrifuge tube, which was spun at 3000 rpm for 3 minutes. The supernatant was gently aspirated without disturbing the cell pellet, which was then resuspended in 4mL of new α-MEM media. Ten µL of cell media was used on a hemocytometer for calculating cell density.

Adhesion, Shaping, and Spreading

Assessing the adhesion as well as shaping or spreading of the pre-osteoblasts on the surfaces suggests an affinity and biocompatibility with the modified surfaces. The greater number of adhesive points as well as spreading of the cells laterally with extensions is an indication that the cells react well with the surface.

Preparing the discs for incubation was conducted under a hood. Titanium discs that were previously conditioned and glass discs were placed in the 48-well plate and covered with 70% ethanol for 30 minutes under UV light. The ethanol was aspirated and the wells with discs were covered with 10% BSA (Thermo Scientific, Logan, UT) and incubated at 37°C for 30 minutes. The wells were then aspirated and rinsed four times with HBSS for 2-3 minutes each.

Cell counting with the hemocytomer was used to calculate the dilutions needed for 2000 MC3T3-E1 cells to be allocated to each well with 0.5mL of media. After each titanium or glass disc was covered with media, they were incubated at 37°C for either 2 or 4 hours. After 2 or 4 hours, the plate was removed from the incubator and media was aspirated gently, rinsed with HBSS, aspirated, and fixed with 4% paraformaldehyde solution (PFA) (Fisher Scientific, Fair Lawn, NJ) for 15 minutes at room temperature. After the PFA was aspirated, it was rinsed three times with 1x phosphate buffered solution (PBS) (Lonza, Walkersville, MD) and was left in the last rinse of PBS at 4°C overnight until staining with fluorescence.

Triple-fluorescent labeling was used to evaluate three important components of the cells simultaneously. DAPI is a known label for nuclear DNA by binding to the A-T rich regions,[26] which was used to identify the number and location of cells with the cell

adhesion/shaping and proliferation assays. Rhodamine phalloidin binds F-actin of the cytoskeleton[27] and was used to display cellular shaping and extensions. Vinculin is a cytoskeletal protein that is involved in the signaling from the ECM to intracellular cytoskeleton and thus labels contact or adhesion points.[28]

Titanium discs were then transferred onto paraffin wax with their treated surface towards the paraffin to reduce the reagents needed to cover the discs (Figure 3). Glass was treated with antibodies while in their separate plate wells. Cells were lysed with PBS+0.3% TX-100 for 10 minutes, followed by aspiration, and incubated for 30 minutes with IF solution (1.5g BSA + 5mL 10x PBS + 0.5mL 2M $MgCl_2$+150µL Tween20+ distilled water to a final volume of 50mL) at room temperature. In a dark room, the primary antibody (monoclonal anti-vinculin made in mouse) was diluted 1:500 in IF solution and was pipetted to cover the discs that incubated for 3 hours at 37°C. The discs were covered with aluminum foil and damp paper towel to reduce light exposure and prevent evaporation of antibody solution. The discs were then rinsed 3 times with PBS+0.1%TX-100 for 5 minutes each. After aspiration of the last rinse, Alexa-Fluor conjugated secondary antibody (GMM488) (Invitrogen, Eugene, OR) was diluted 1:600 in IF solution, DAPI (4',6-diamidino-2-phenylindole, dilactate) (Invitrogen, Eugene, OR) was diluted 1:1500 in IF solution, and rhodamine phalloidin (TRITC) (Invitrogen, Eugene, OR) was diluted 1:5000 with IF solution. These antibody solutions were pipetted to cover the discs and incubated for 1 hour and 15 minutes at 37°C with aluminum foil and damp paper towel coverings. After incubation, the discs were washed again for 3 times with PBS+0.1%TX-100 for 5 minutes each, dried, and stored. The

discs were stored in 48-well plates sealed in paraffin wax and aluminum foil at 4°C until viewing fluorescence with microscope.

Figure 3: Diagram of Immunofluorescent Incubation System

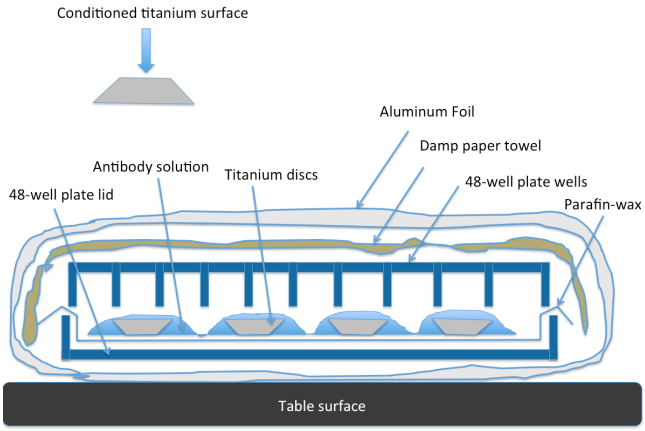

Diagram of titanium discs incubating "up-side-down" over paraffin-wax to reduce the quantity of antibody solution needed to cover conditioned side of discs. The diagram also displays the paraffin wax was placed over a new well plate lid, while the plate wells acted like a lid. Damp paper towel was placed over the plate to reduce evaporation of the antibody solution and the aluminum foil sealed the plate from light during the incubation period.

Cellular fluorescence were visualized with a Nikon Eclipse E800 Light microscope with a Nikon super high-pressure mercury lamp and MetaMorph V6.2r2 (Universal Imaging Corp., Buckinghamshire, UK) software. Exposure times for the different fluorescent stains (DAPI, rhodamine phalloidin, Vinculin) were 5000-8000 milliseconds (ms) for rhodamine phalloidin (red-orange), 3000-6000 ms for Vinculin (green), and 200-800 ms for DAPI (blue). Magnification of 10x was used to view cells incubating for 4 hours with DAPI or rhodamine phalloidin to evaluate cell proliferation with 3 random pictures taken for each disc and 3 discs sampled per surface group. Magnification of 20x was used for viewing the cell sSNa15ing and spreading with

rhodamine phalloidin of both 2 and 4 hour samples with 1 picture per disc and 3 discs sampled per surface group. Magnification of 40x was used to view cell adhesion with DAPI, rhodamine phalloidin, and Vinculin, of cells at both 2 and 4 hours with 1 random sample picture per disc and 3 discs viewed per surface group. The 40x views had individual photos taken of each fluorescent stain and had them combined using imageJ 1.45e (National Institute of Health, USA) software. ImageJ was also used to quantify viewing scale by referencing pixels to previously determined distances (Table 3).

Table 3: Conversion Between Pixels and Distance

Objective	Calibration size (µm)	Region size (pixels)
10x	250	241
20x	250	475
40x	250	976

Table showing associated pixels on ImageJ software to distances of microscope viewing on Nikon Eclipse 800 microscope at different magnification objectives.

Proliferation

While under the hood, titanium discs that were previously conditioned and glass discs were placed in the 48-well plate and covered with 70% ethanol for 30 minutes under UV light. The wells were then aspirated and rinsed four times with HBSS for 2-3 minutes each.

Cell counting with the hemocytometer was used to calculate the dilutions needed for 2000 MC3T3-E1 cells to be allocated to each well with 0.5mL of complete media. After each titanium or glass disc was covered with media, they were incubated at 37°C for 24, 48, or 72 hours. After 1, 2, or 3 days, the specific plate was removed from the incubator and media was aspirated gently, rinsed with HBSS, aspirated, and fixed with

4% PFA for 15 minutes at room temperature. After the PFA was aspirated, it was rinsed three times with 1x PBS and was left in the last rinse of PBS at 4°C until staining with fluorescence.

Samples had PBS aspirated, and then incubated at room temperature for 10 minutes with PBS+0.3% TX-100. The discs were then transferred to an "up-side-down" paraffin-wax tray (Figure 3) and incubated with 1:1000 DAPI (360nM) for 15 minutes in a dark environment (covered with aluminum foil). After incubation, discs were rinsed with distilled water and stored in the dark at 4°C refrigerator until observing. Fluorescence was viewed with a Nikon Eclipse E800 Light microscope with a Nikon super high-pressure mercury lamp and MetaMorph V6.2r2 software. The mean proliferations of each surface group and incubation time were calculated by averaging the number of nuclei using ImageJ software of 3 random views per disc and 3 discs were surface modified group.

Differentiation

Titanium discs that were previously conditioned and glass discs were placed in the 48-well plate and covered with 70% ethanol for 60 minutes under UV light. The wells were then aspirated and rinsed four times with HBSS for 2-3 minutes each.

Cell counting with the hemocytometer was used to calculate the dilutions needed for 50,000 MC3T3-E1 cells to be allocated to each well with 0.8mL of complete media. After each titanium or glass disc was covered with media, they were incubated at 37°C for 7, 14, or 21 days. After confluence and the media was changed to osteogenic media (α-MEM + 10% FBS + 1% Penn-step + 50μg/mL L-ascorbic acid + 10nM β-glycerol

phosphate), which was aspirated gently and replaced every 2-3 days until incubation was complete. After 7, 14, or 21 days, the specific plate was removed from the incubator and media was transferred into an eppendorf tube and stored at -20°C for the osteocalcin assay. The discs were then rinsed gently with PBS for 5 minutes. After aspiration of PBS, ALP lysis buffer (distilled water with 1% TritonX-100, 0.1mM $MgCl_2$, 150mM tris; to pH: 10.5) with Halt protease inhibitor (100x) (Thermo Scientific, Rockford, IL) was incubated on ice for 10 minutes. The discs were then scrapped and collected into an eppendorf tube. The collected cells were spun at 3000rpm for 10 minutes at 4°C. Supernatant was transferred to a new eppendorf tube and stored at -20°C for measuring ALP and total protein.

Total Protein Assay

The purpose for this assay was to assess the total protein of each sample, which is related to the total number of cells present in each sample. Differentiation assays could then be related to the total protein in their respective sample to establish a more proportionate differentiation expression per cell. Bio-Rad DC Protein Assay reagents were purchased (Bio-Rad Laboratories, Hercules, CA) and Bio-Rad Microplate Assay protocol was followed. Reagent A' is a mixture of 20µL reagent S and 1mL of reagent A. Serial dilutions of lyophilized BSA in concentrations of 0, 0.2, 0.4, 0.6, 0.8, 1.0, 1.2, 1.42mg/mL were prepared in ALP lysis buffer. In a 96-well microtiter plate, 5µL of standards or samples were combined with 25µL of reagent A' and 200µL reagent B. After 15 minutes of incubation with gentle agitation, absorbances were read at 650nm on Beckman Coulter AD340 Spectrophotometer at 37°C. After subtracting the blank

(0mg/mL) from absorbances, a standard linear trend-line was established based on the serial dilutions and used to calculate total protein concentrations (mg/mL) of each incubated disc sample.

Alkaline Phosphatase

Alkaline phosphatase is an enzyme that hydrolyzes pyrophosphate, which is believed to play a role in promoting osteoid mineralization.[29] This is also the first restriction point in the differentiation of osteoblasts. As proliferation of the pre-osteoblasts decreases, ALP expression increases for the maturation of the osteoid. Thus, ALP is an established marker for early osteoblastic differentiation.[30,31] Freshly prepared 100µL AMP reaction solution (22.5µL AMP (2-amino-2-methyl-1-propanol) diluted first in 1:4 in distilled water) + 12µL 2M $MgCl_2$ + 2 20mg p-Nitrophenyl phosphate tablets + 10mL distilled water) was combined with 2µL sample supernatant into a new 96-well microtiter plate. This was incubated at 37°C for 60 minutes and then 25µL of 2M NaOH was added per well and absorbance was read at 405nm on Beckman Coulter AD340 Spectrophotometer at 37°C. Absorbances had mean blank (AMP reaction solution alone) subtracted from it and then had ALP activity was determined relative to total protein concentration (see *Total Protein Assay*).

Osteocalcin

The second restriction point in osteoblastic differentiation is when maturation of the osteoid ends and mineralization begins. Osteocalcin is a vitamin-K dependent, calcium binding protein involved in osteoid mineralization and is a marker for late

osteoblastic differentiation.[30-32] Biomedical Technologies Inc. (Stoughton, MA) mouse osteocalcin EIA Kit was obtained and their protocol was followed. Standard stock dilutions of osteocalcin of 0, 1.56, 3.12, 6.25, 12.5, 25, and 50ng/mL were made with stock buffer. Standard dilutions and samples (25µL each) were pipetted into individual microtiter plate wells and combined with 100µL osteocalcin antiserum, sealed, and incubated at 4°C for 20 hours. Wells were washed with phosphate-saline buffer, and then 100µL Steptavidin-Horseradish Peroxidase was added, agitated, and incubated for 30 minutes. Wells were washed with phosphate-saline buffer and then 100µL substrate mixture (TMB and hydrogen peroxide solutions) was added and incubated in the dark at room temperature for 15 minutes. Stop solution (100µL) was added to each well, agitated, and measured absorbances at 450nm in Beckman Coulter AD340 Spectrophotometer at 37°C. The mean blank (0ng/mL) was subtracted from standards and samples. The natural log of absorbances for the standards were plotted against concentrations and the trend-line was used to calculate osteocalcin levels (ng/mL) of each experimental sample. The osteocalcin levels relative to total protein concentration (see *Total Protein Assay*) were determined for each sample.

Statistical Evaluation

Comparisons between surface groups for contact angle, proliferation, and differentiation, were conducted at each time point. Statistical comparisons involved a one-way ANOVA and Bonferroni pairwise multiple comparisons using SPSS (19.0, IBM, USA) with a confidence interval of 95%.

RESULTS

Surface Characterization: DRIFTS

Diffuse reflectance infrared Fourier transform spectroscopy (DRIFTS) was utilized to verify the presence of the ELPP-coating on the titanium surfaces. DRIFTS was also performed on at least one ELPP-coated titanium sample before each assay to verify the successful coating of biopolymers. Only one representative DRIFTS spectrum of each titanium surface group is shown in Figure 4. Those titanium surfaces that had ELPPs covalently bonded to the surfaces showed peaks for their hydroxyl and two amide groups (B). The titanium surfaces without ELPPs bonded to the surfaces only showed a peak at ~2300cm^{-1} consistent with carbon dioxide (B), which was also present for samples with ELPPs (A).

Figure 4: DRIFTS

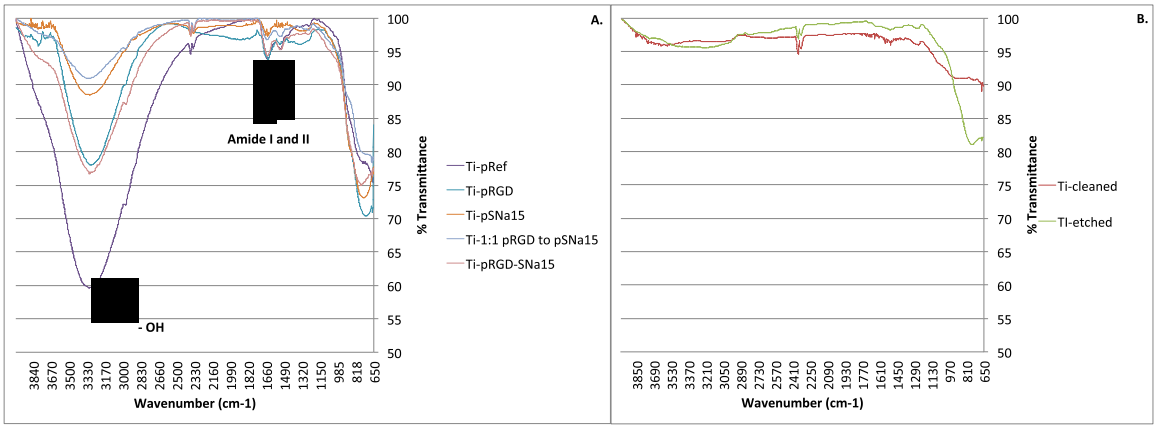

DRIFTS results showing the presence of peaks for a hydroxyl group, and two amide groups for samples with bioactive biopolymers (A), while the samples without biopolymers show only peaks for the presence of carbon dioxide and environmental traces (B).

Surface Characterization: Contact Angle

Contact angle measurements were obtained for 3 discs per titanium sample group shortly (<30 minutes) after coating was complete or discs were re-cleaned with cold distilled water, then acetone, and then dried. The contact angles were measured every second for 60 seconds immediately after distilled water droplet contacted the surfaces. Cleaned-titanium and etched-titanium showed a significantly lower contact angle compared to the ELPP-coated titanium surfaces immediately after the droplet contacted the surface ($p<0.05$) (Figure 5AB). All of the ELPP-coated titanium surfaces showed decreasing contact angles over time but Ti-pRGD, Ti-pRef, and Ti-pRGD-SNa15 displayed the least change (Figure 5A). The final contact angle of Ti-pSNa15 and Ti-1:1 pRGD to pSNa15 showed significantly lower contact angles compared to Ti-pRGD, Ti-pRef, and Ti-pRGD-SNa15 ($p<0.05$) (Figure 5C).

Figure 5: Contact Angle

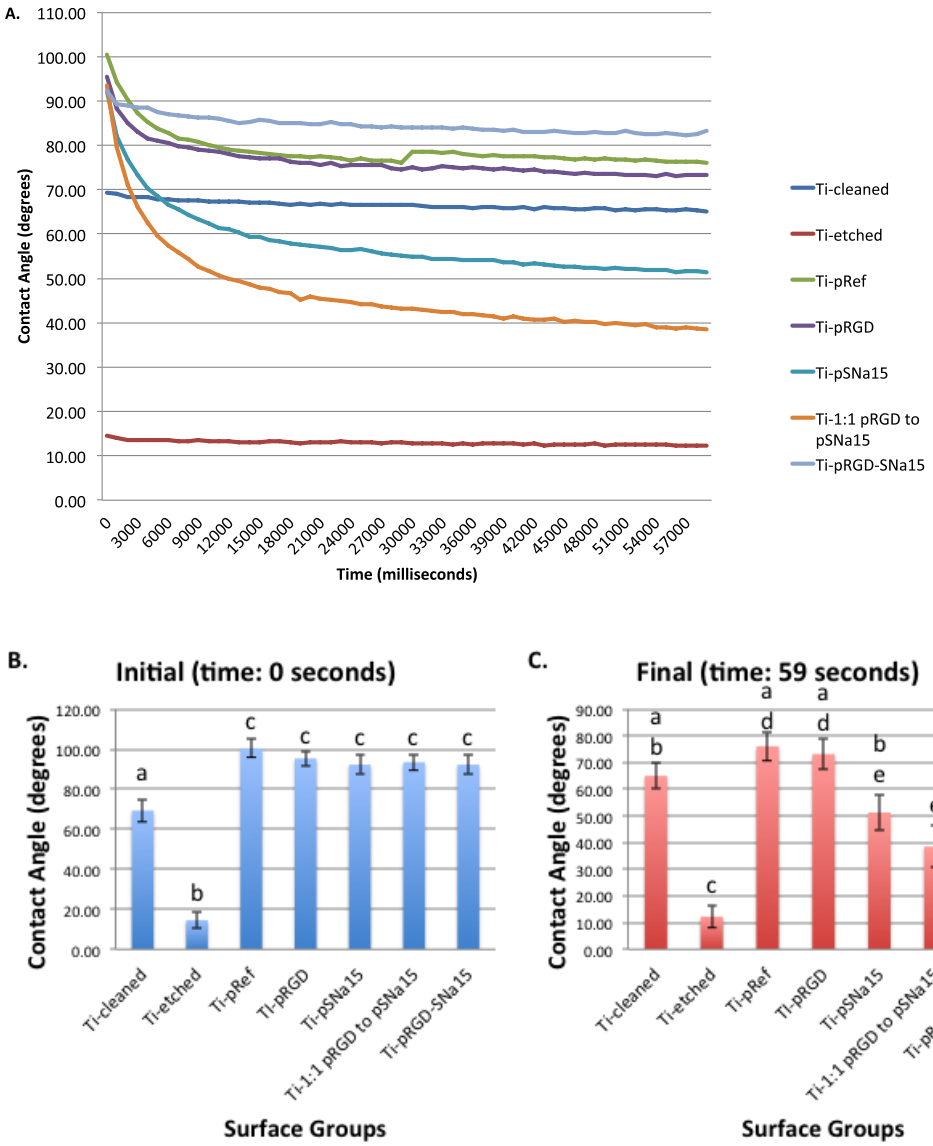

Mean dynamic contact angles of distilled water on coated or conditioned titanium discs over 60 seconds of observation (A) as well as bar-graphs showing initial and final contact angles with standard deviations (B, C). Different letters indicate statistical difference ($p<0.05$) between surface groups within the same time points (B, C).

Cellular Adherence: Adhesion

After 2 hours of incubation, only pre-osteoblasts on cleaned-titanium, Ti-pSNa15, and Ti-pRGD-SNa15 demonstrated clear focal adhesion points (As indicated in green in

Figure 6). Although incubating cells on Ti-pSNa15 and Ti-pRGD-SNa15 displayed clear focal adhesion points after 2 hours, these cells also displayed limited cellular extensions compared to all other surfaces (Figure 6). After 4 hours of incubation, there were greater numbers of focal adhesion points (Figure 7) when compared to after 2 hours (Figure 6). The number and location of focal adhesion points could not be quantified but a general impression noted greater numbers with samples from the Ti-pRGD sample after 4 hours (Figure 7).

Figure 6: Adhesion at Two Hours

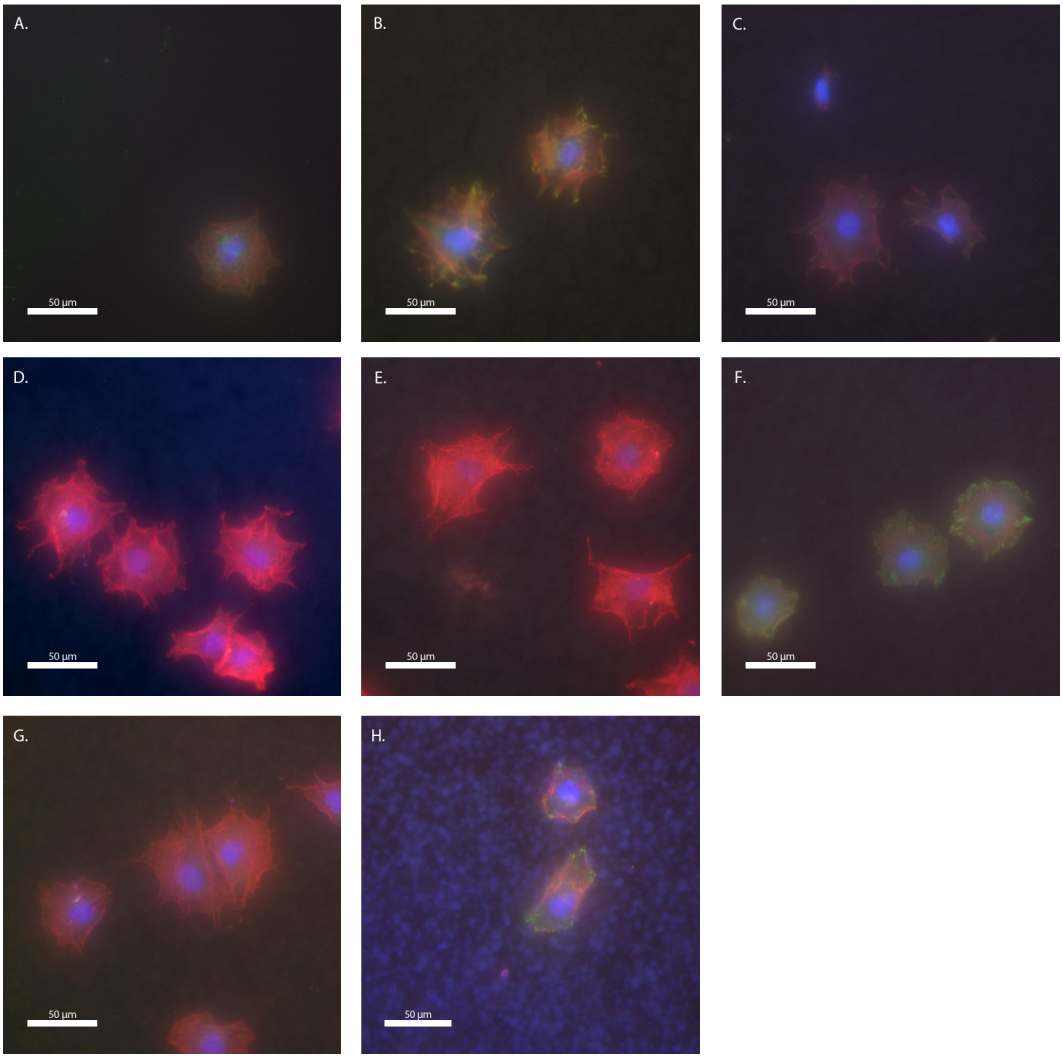

Pre-osteoblastic (MC3T3-E1) adhesion of BSA-conditioned titanium-surfaces with or without ELPPs assessed with immunofluorescence triple staining analysis at 40X magnification on a light microscope after 2 hours of incubation. (A) Glass (positive control) (B) Titanium-cleaned (negative control) (C) Titanium-etched (D) Ti-pRef (E) Ti-pRGD (F) Ti-pSNa15 (G) Ti-1:1 pRGD to pSNa15 (H) Ti-pRGD-SNa15.

Figure 7: Adhesion at Four Hours

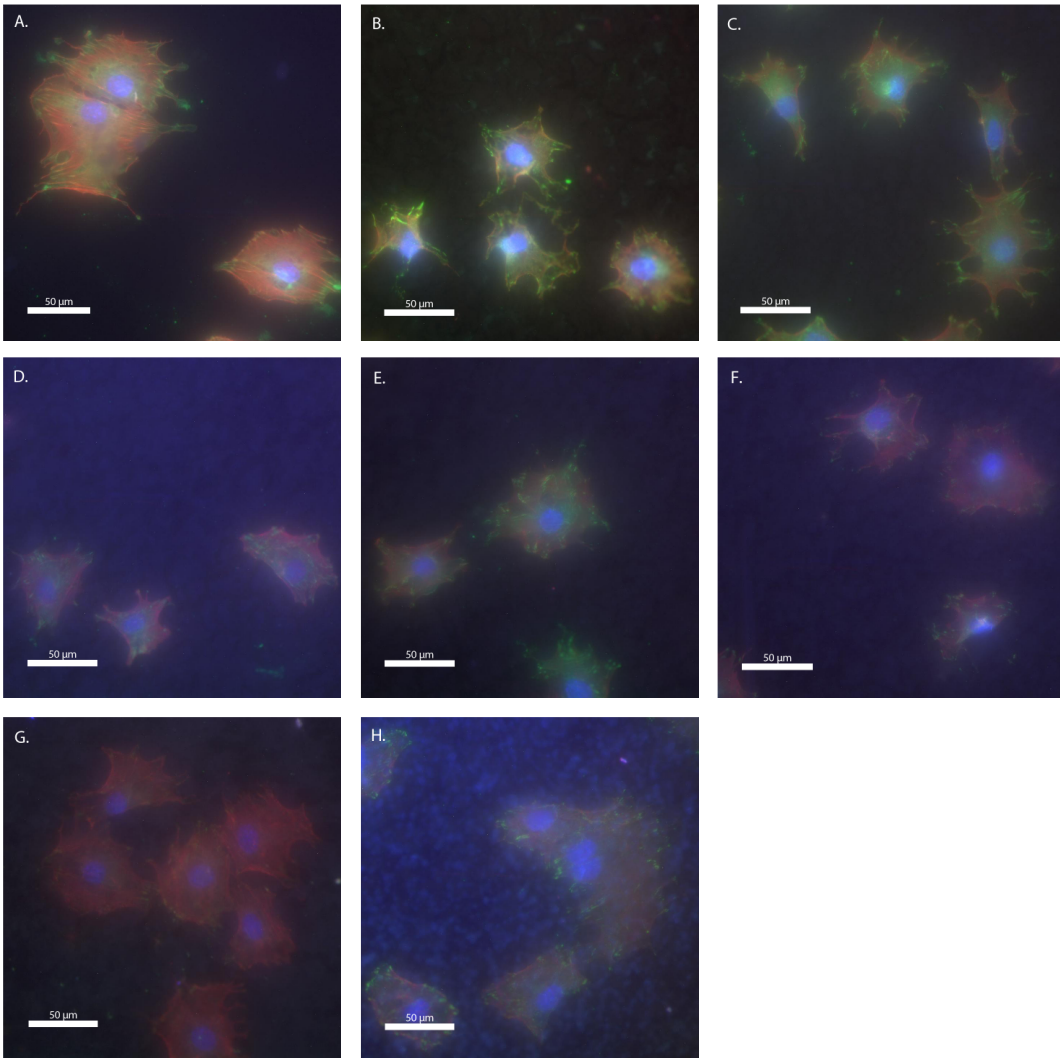

Pre-osteoblastic (MC3T3-E1) adhesion of BSA-conditioned titanium-surfaces with or without ELPPs assessed with immunofluorescence triple staining analysis at 40X magnification on a light microscope after 4 hours of incubation. (A) Glass (positive control) (B) Titanium-cleaned (negative control) (C) Titanium-etched (D) Ti-pRef (E) Ti-pRGD (F) Ti-pSNa15 (G) Ti-1:1 pRGD to pSNa15 (H) Ti-pRGD-SNa15.

Shaping and Spreading

After 2 hours of incubation, all surface groups demonstrated rounded cellular shapes with limited extensions (Figure 8). Pre-osteoblastic cells improved cellular spreading between 2 and 4 hours of incubation as denoted by a greater number and longer extensions of their cells and more cells with a stellate appearance (Figures 8 and 9). There appeared little, if any, qualitative differences between the spreading and shaping of pre-osteoblasts on each surface group at either observation period (Figure 9).

Figure 8: Cell Shaping and Spreading at Two Hours

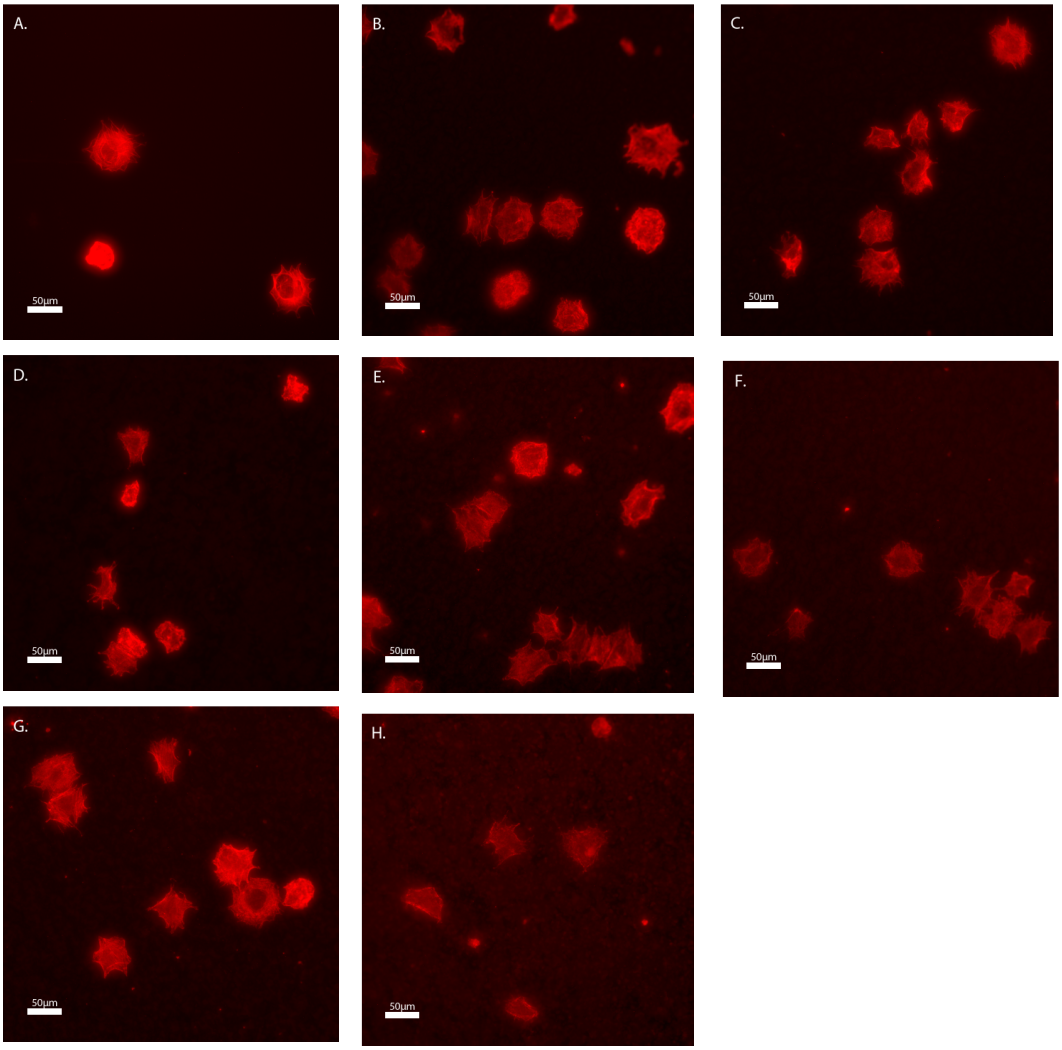

Cell shaping and spreading of pre-osteoblastic cells (MC3T3-E1) on coated or conditioned titanium surfaces with F-actin immunofluorescence staining at 20X magnification on a light microscope after 2 hours of incubation. (A) Glass (positive control) (B) Titanium-cleaned (negative control) (C) Titanium-etched (D) Ti-pRef (E) Ti-pRGD (F) Ti-pSNa15 (G) Ti-1:1 pRGD to pSNa15 (H) Ti-pRGD-SNa15.

Figure 9: Cell Shaping and Spreading at Four Hours

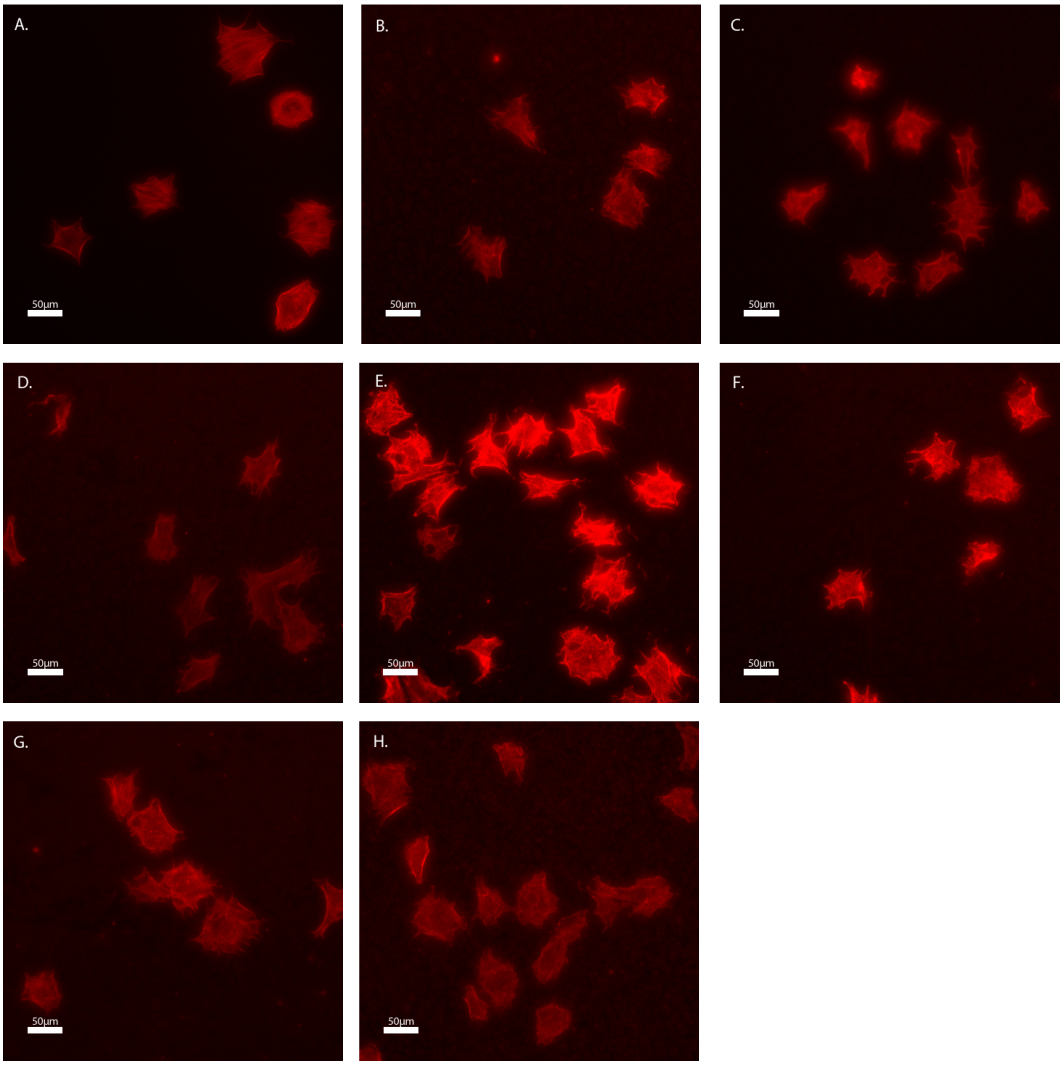

Cell shaping and spreading of pre-osteoblastic cells (MC3T3-E1) on coated or conditioned titanium surfaces with F-actin immunofluorescence staining at 20X magnification on a light microscope after 4 hours of incubation. (A) Glass (positive control) (B) Titanium-cleaned (negative control) (C) Titanium-etched (D) Ti-pRef (E) Ti-pRGD (F) Ti-pSNa15 (G) Ti-1:1 pRGD to pSNa15 (H) Ti-pRGD-SNa15.

Cellular Proliferation

All of the surface groups showed increasing pre-osteoblastic (MC3T3-E1) cell numbers during the first 3 days of incubation. Groups with the highest numbers after 1 day of incubation included Ti-pRGD, while pSNa15 had significantly lower numbers

after 1 day compared to glass, Ti-cleaned, Ti-pRef, and Ti-pRGD ($p<0.05$). After 2 days of incubation the groups Ti-pRGD-SNa15 had significantly greater mean cell numbers than glass, Ti-etched, and Ti-pRef ($p<0.05$), while no other groups were significantly different ($p>0.05$). On day 3 of incubation, the greatest mean cellular number was noted on Ti-pRGD and Ti-pSNa15 surfaces, with a significantly greater cell number compared to glass ($p<0.05$). Ti-pRGD was also significantly greater than Ti-etched after 3 days of incubation ($p<0.05$). Variability of cell number counts within the same incubation-period and surface groups increased with increasing days of incubation (Figure 10).

Figure 10: Proliferation

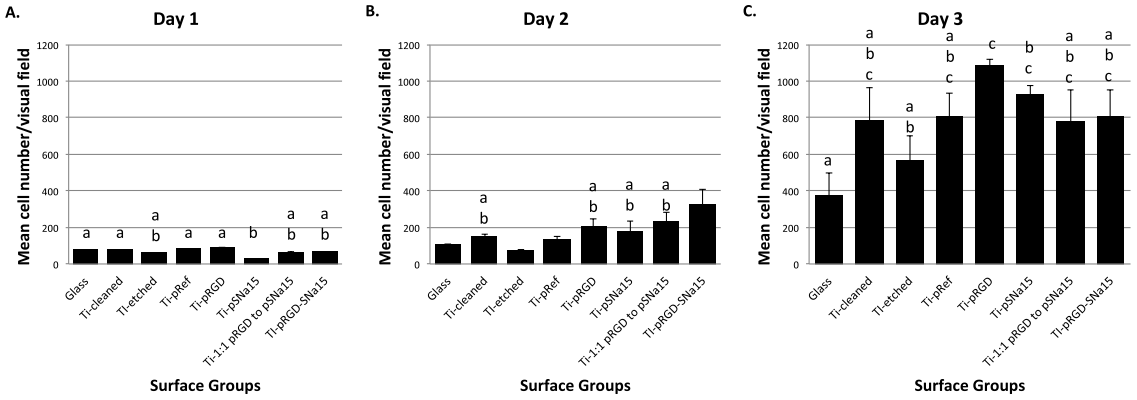

(A-C): Proliferation of MC3T3-E1 cells on coated or conditioned titanium and glass surfaces after incubation for 1, 2, and 3 days based upon cell number per visual field at 10x magnification on a light microscope. Different letters indicate statistical difference ($p<0.05$) between surface groups within the same incubation periods.

Osteoblastic Differentiation: Alkaline Phosphatase

Alkaline phosphatase activity was noted to be the highest for most groups after 14 days or 21 days of incubation except for cleaned titanium. After 7 days of incubation, all ELPP-coated titanium samples with pRGD (Ti-pRGD, Ti-1:1 pRGD to pSNa15, Ti-pRGD-SNa15) had significantly lower ALP activity compared to all other surfaces

($p<0.05$) (Figure 11B). Aside from the positive control at day 14, there were no statistically significant differences between ALP activity between any of the samples after 14 or 21 days of incubation ($p<0.05$) (Figure 11C and 11D).

Figure 11: Alkaline Phosphatase Activity

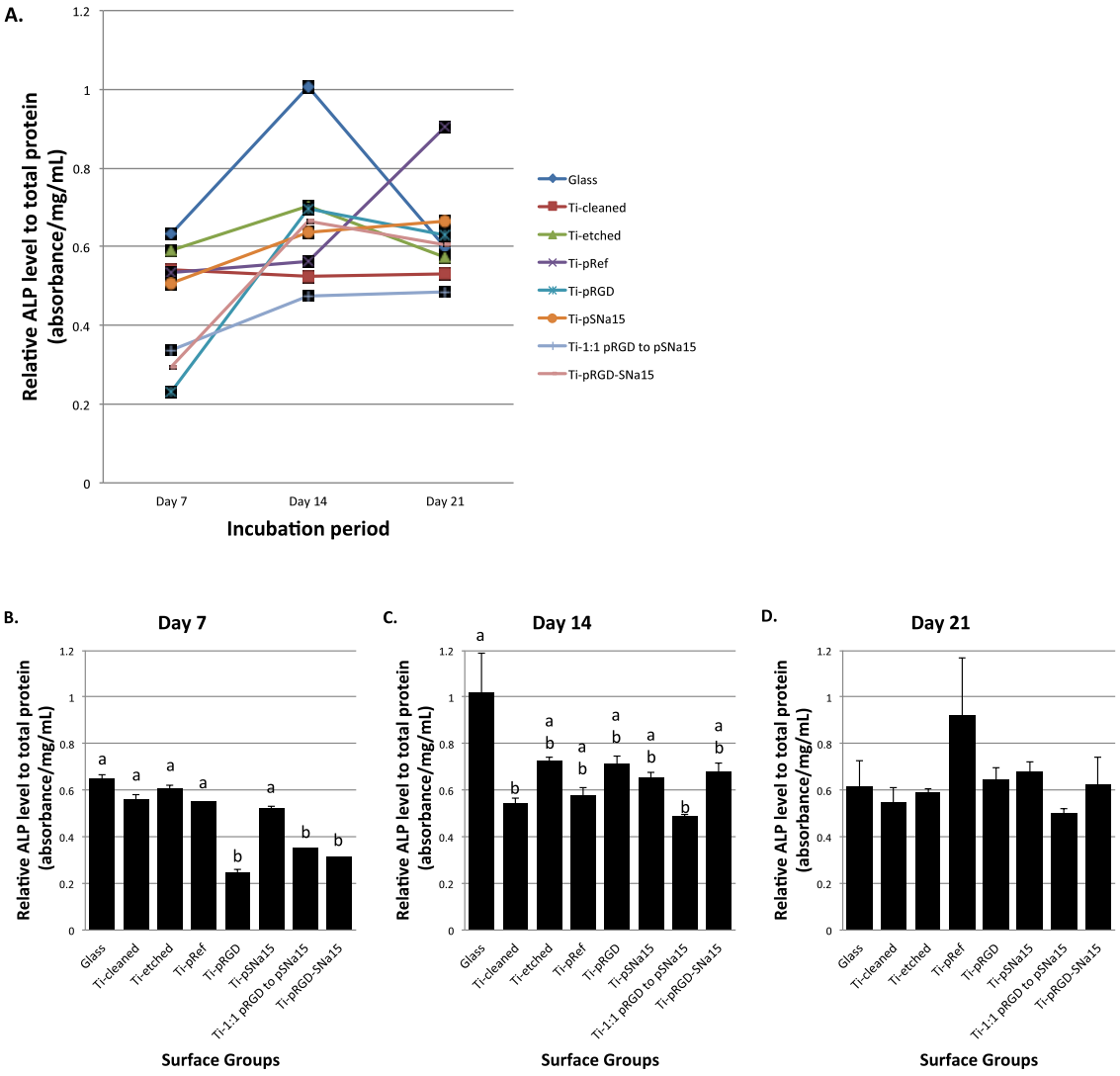

(A-D): Alkaline phosphatase (ALP) activity (mean absorbance at 405nm / total protein concentration (mg/mL)) of MC3T3-E1 cells incubated for 7, 14, or 21 days on different titanium surfaces and glass (positive control). Temporal changes in ALP activity between different surface groups are shown in a line-graph (A). Bar-graphs compare ALP activity at each incubation period and different letters indicate statistical difference ($p<0.05$) between surface groups within the same incubation periods (B, C, D).

Osteocalcin

Osteocalcin levels were determined to be greatest after 21 days of incubation for most groups. The only exceptions include Ti-pRGD and Ti-pRGD-pSNa15, which displayed their highest relative OCN levels at 14 days and decreased their OCN levels at 21 days (Figure 12A). When comparing to the positive control (glass), titanium surfaces coated with a combination of both biomimetic ELPPs (Ti-1:1 pRGD to pSNa15 and Ti-pRGD-SNa15) had significantly lower relative OCN levels after 14 days. Ti-pRGD and Ti-pRGD-SNa15 displayed significantly lower OCN levels after 21 days of incubation compared to the positive control (glass). Aside from these decreased OCN levels found in the forementioned ELPP-coated titanium surfaces compared to the positive control, there were no significant differences in OCN levels between ELPP-coated titanium surfaces at any incubation period ($p>0.05$) (Figure 12).

Figure 12: Osteocalcin Level

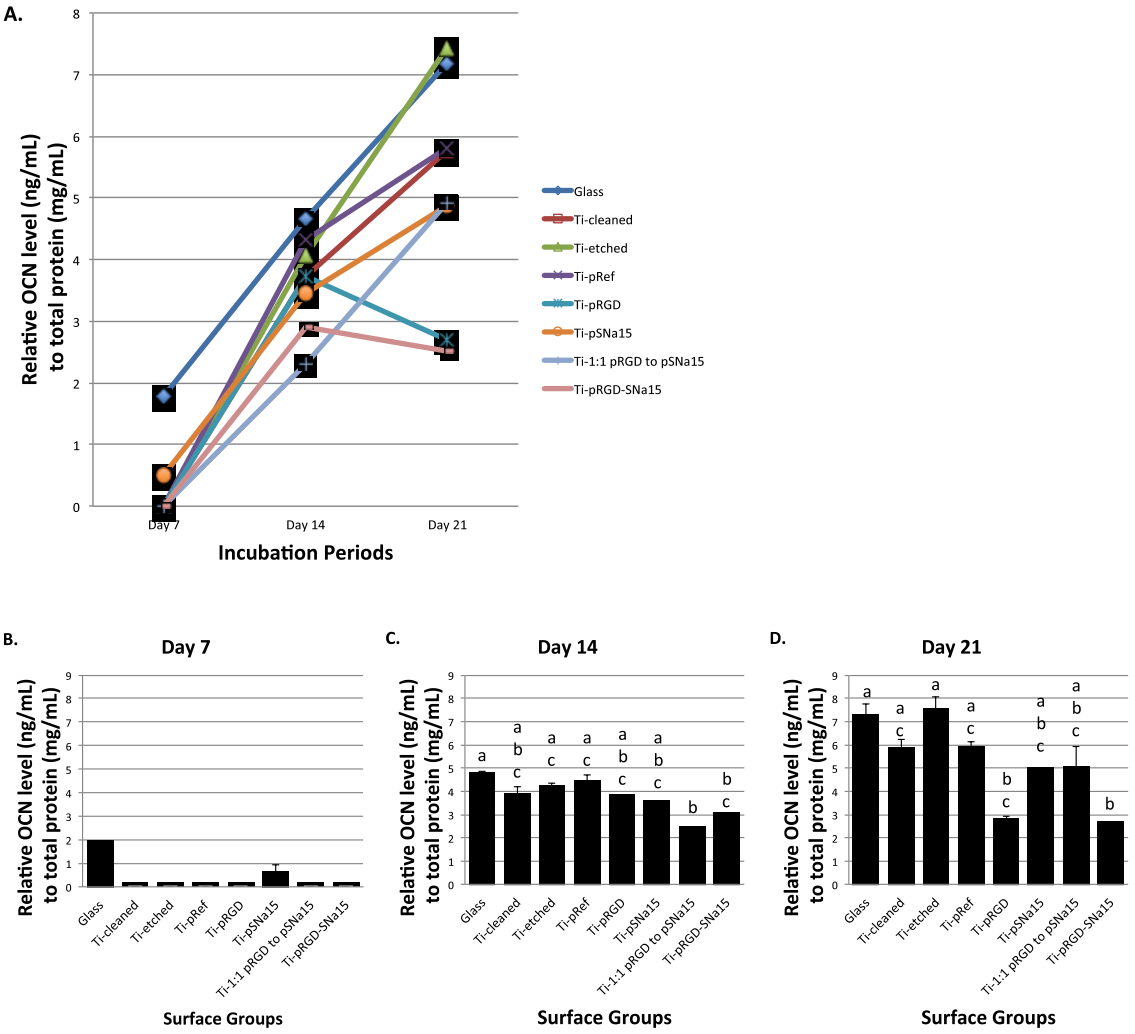

(A-D): ELISA results of osteocalcin (OCN) levels (ng/mL) relative to total protein concentration (mg/mL) of MC3T3-E1 cells incubated for 7, 14, or 21 days on different titanium surfaces and glass (positive control). Temporal changes in OCN levels between different surface groups are shown in a line-graph (A). Bar-graphs compare OCN levels at each incubation period and different letters indicate statistical difference ($p<0.05$) between surface groups within the same incubation periods (B, C, D). Statistical significance was not determined between sample groups at Day 7 because most surfaces had lower OCN levels (absorbance) than the measured blank.

DISCUSSION

The purpose of this study was to evaluate the benefits of covalently coating titanium with two bioactive elastin-like peptide polymers (pRGD and pSNa15) in regards to osseointegration-related outcomes. Our results indicate that there is a distinct difference in the wettability between titanium surfaces with a 1:1 molar ratio of pRGD to pSNa15 and a titanium surface coated with single molecules of pRGD-SNa15. Despite this surface characteristic difference, these two titanium surfaces did not significantly differ in terms of pre-osteoblastic adhesion, proliferation, and differentiation. Late-stage differentiation of the Ti- 1:1 molar ratio of pRGD to pSNa15 displayed a more normal pattern compared to the Ti-pRGD-SNa15. These titanium surfaces with both bioactive ELPPs also resulted in similar osteoblastic responses compared to titanium surfaces with only one ELPP (Ti-pRGD or Ti-pSNa15). Of interest is that Ti-pRGD related similarly to Ti-pRGD-SNa15, while Ti-pSNa15 related with Ti-1:1 pRGD to pSNa15 in terms of surface wettability and late-stage differentiation.

Contact Angle

Contact angle was used to evaluate the wettability of the modified titanium surfaces. Those surfaces with hydrophobicity would have a greater contact angle, while those with a lower contact angle would be characterized as hydrophilic. The hydrophilicity of titanium is important because previous research has indicated that a hydrophilic surface of dental implant is associated with improve tissue integration.[33] Etched-titanium demonstrated significantly greater hydrophilicity compared to all other groups at all time points ($p<0.05$) (Figure 5). This is consistent with previous studies[25]

and with the notion that etching titanium results in activated hydroxyl groups that makes the surface extremely hydrophilic.[33] Elastin-like polymers have only mildly hydrophobic components consisting of the proline and valine side chains.[34] Most of the ELPPs-coated titanium samples (except Ti-pRGD-HAP) showed a temporal change in contact angle from a hydrophobic to more hydrophilic state (Figure 5). This is believed to be due to conformational changes of the elastin-like polymer to hide the hydrophobic components and display the hydrophilic components of this amphiphilic molecule.[23] Those peptide-polymer-coated surfaces containing the SNa15 motif demonstrated significantly greater hydrophilicity compared to peptide-polymer surfaces without ($p<0.05$) (Figure 5). This is likely due to the acidic and polar properties of the DDDEE amino acids found on the N-terminus of the statherin-drived peptide.[14] Of the ELPP–coated surfaces, the titanium surface with 1:1 molar ratio of pRGD and pSNa15 displayed the greatest hydrophilicity at the final contact angle measurement. On the other hand, the titanium surface with one molecule of both bioactive peptides (Ti-pRGD-SNa15) showed the greatest hydrophobicity (Figure 5). We cannot definitively explain this result but can only speculate the ELPP-coated titanium with one molecule of pRGD-SNa15 cannot conform to hide the hydrophobic or display the hydrophilic (i.e. DDDEE) components effectively. The inability of Ti-pRGD-SNa15 to display the SNa15 motif could explain why there is no statistically significant difference in final contact angle compared to the titanium surface with only elastin-like polymer (Ti-Ref) or with only pRGD (Ti-pRGD) ($p>0.05$) (Figure 5).

In conclusion, a titanium surface with two bioactive ELPPs (1:1 molar ratio of pRGD and pSNa15) was significantly more hydrophilic than one ELPP of both bioactive

peptides (Ti-pRGD-SNa15) ($p<0.05$). The titanium surface with two bioactive ELPPs (1:1 molar ratio of pRGD to pSNa15) was significantly more hydrophilic than a titanium surface with pRGD ($p<0.05$), but not more hydrophilic than with pSNa15 ($p>0.05$).

Cell Adhesion

Assessing cell adhesion and shaping is important in determining the affinity of cells to the novel material surface. Focal adhesion points (as indicated in green in Figures 6 and 7) are areas where the cells have bound the intracellular actin cytoskeleton to the extracellular surface via trans-membrane glycoproteins (Integrins).[9] After integrin-binding, the actin cytoskeleton condenses and binds structural proteins like vinculin.[35] Establishing this cellular attachment is important in not only cellular anchorage, but also in influencing proliferation, differentiation, and apoptosis by activating signaling cascades.[8,35] Cells that display more focal adhesion points or that spread with elongated cellular extensions are considered to have a better cellular affinity for the surface. In our study, triple-fluorescence staining allowed for visualization of the nucleus, actin, and vinculin components. While all of the samples showed numerous focal adhesion points after 4 hours of incubation, the titanium surface with pRGD (Ti-pRGD) demonstrated a trend of greater numbers (Figure 7). Co-immobilizing both biomimetic peptide polymers does not significantly improve cellular adherence and actually detracts from adherence compared to titanium coated with only pRGD. There appears to be no measurable difference in the focal adhesion points between titanium surfaces coated with both ELPPs (Ti-pRGD-SNa15 versus Ti-1:1 pRGD to pSNa15).

Shaping of the cells is also an important measure in the cells affinity for the new surface. Similar to the results from assessing focal adhesion points, the cellular shaping and extensions were comparable between surface groups after 2 (Figure 8) and 4 hours (Figure 9). Qualitative evaluation of the cellular spreading and extensions revealed that etched-titanium showed slightly more spreading and longer extensions (Figure 9). From comparing the cellular spreading of the titanium surfaces with ELPPs, no specific group appeared to promote more spreading than the others. At the same time, all of the groups demonstrated some degree of spreading (Figure 9). While no specific ELPP-coated titanium surface appeared superior in terms of promoting cellular spreading, all of these surfaces facilitated cellular attachment. Thus, these results indicate each of these ELPP-coated titanium surfaces are biocompatible and pre-osteoblastic cells show an affinity for each surface group.

Cells frequently attach to ECM proteins via integrin-RGD binding, which would give evidence that titanium surfaces containing pRGD would have improved cellular adhesion (more focal adhesion points) and greater cellular spreading. Those samples with pRGD appeared to demonstrate a trend in greater numbers of focal adhesion points (Figure 7), but showed similar cellular spreading compared to other surfaces (Figures 8 and 9). As described previously, these ELPPs on titanium surfaces undergo conformational changes upon exposure to a water-based environment. The ELPP molecules change to present the hydrophilic and hide the hydrophobic portions of the amphiphilic structure. During these changes, the RGD peptide may be hidden from the environment or negated from binding osteoblastic integrins. This is a common occurrence, as only a minority of previously described proteins with RGD mediate

cellular attachment.[8] To avoid the problems associated with conformational changes of long elastin-like polymers hiding biomimetic peptide sites, other researchers have investigated short peptides. Furthermore, elastin-like polymers may be beneficial for biomimetic materials embedded in soft tissue that require the mechanical strength and flexibility of elastin,[22,34] titanium implants may not require this characteristic. Instead of using elastin-like polymers to bind the peptides to titanium, only the biomimetic peptide was covalently bound to the titanium via a similar silanization treatment. While this technique is novel, recent results indicate titanium surfaces coated with RGD-containing peptides showed greater cellular extensions compared to plain titanium.[36] Unpublished research from our laboratory has also found that co-immobilizing two different biomimetic peptides can be accomplished using this short peptide technique.[37] Thus, our results demonstrated titanium surfaces coated with pRGD alone may improved cell adhesion, but titanium coated with pSNa15 or co-immobilized with both biomimetic peptide polymers are not superior to control surfaces. Future research into modifying the ELPP structure may demonstrate a structure with more accessible RGD motifs for improved cellular attachment.

Proliferation

Measuring proliferation is valuable in evaluating the biocompatibility and viability of cells grown on novel bioactive surfaces. Cellular attachment can also influence proliferation by inducing intracellular signaling of the adherent cell.[8,35]

As with our cellular attachment results, pre-osteoblastic proliferation only displayed slight differences between different ELPP-coated titanium groups. Titanium

coated with the pRGD motif had significantly greater cell proliferation after 1 day compared to the titanium surface with pSNa15. Then the Ti-pSNa15 surface showed increasing rates of proliferation, which accounted for the similar cell numbers at day 3 of incubation between the Ti-pSNa15 and Ti-pRGD surfaces ($p>0.05$) (Figure 10). By day 3, the Ti-pSNa15 and Ti-pRGD surfaces had significantly greater cell numbers than the positive control (Glass) ($p<0.05$), but were not different compared to surfaces with both bioactive ELPPs (Ti-1:1 pRGD to pSNa15; Ti-pRGD-SNa15) ($p>0.05$). These results indicate that RGDs demonstrated only a trend in improving cellular proliferation after 3 days of incubation compared to other ELPP-coated titanium surfaces ($p>0.05$) (Figure 10). Overall, there were no differences between ELPP-coated titanium groups after 2 or 3 days of incubation ($p>0.05$) (Figure 10). On the other hand, these proliferation results did demonstrate that each of these modified titanium surfaces are biocompatible to pre-osteoblasts and allow for the viability and proliferation of these cells as similar to cleaned titanium.

Differentiation

We have demonstrated that pre-osteoblasts can adhere to and proliferate on modified titanium surfaces at least as effectively as clean titanium. While the titanium surface with pRGD only showed a trend in improved adhesion and cellular proliferation compared to other modified-titanium surfaces (Figure 8), pRGD and pSNa15 may also impact the differentiation of these adhered pre-osteoblasts.

There are three described phases in osteoblastic development; proliferation, ECM maturation, and mineralization. There are restriction points between these phases that are

represented with specific gene expressions. After the cells come to confluence, there is an increase in alkaline phosphatase activity, which signals the end of proliferation and the beginning of ECM maturation. This phase is important to organize the ECM so that the matrix can be then mineralized. The mineralization phase is signaled by osteocalcin and the development of a mineralized matrix.[30,31]

Our laboratory has noted early differentiation results with ALP from MC3T3-E1 clones to be inconsistent with theoretical results. Our clone of murine pre-osteoblasts (MC3T3-E1) does not appear to produce ALP activity at the normal level, while incubating on any titanium surfaces.[16] Similar behavior has been previously reported[16] and accumulated data in our laboratory confirms this hypothesis. ALP should present with a peaking level at 14 days of incubation, with lower levels at day 7 and 21.[30,31] As depicted by our results, the only surface group with a well-pronounced peak at day 14 is the positive control (Glass) (Figure 9). The ELPP-coated titanium surfaces show a gradual increase from day 7 to either day 14 or 21 but with insignificant differences between ELPP-coated titanium groups ($p>0.05$) (Figures 9C and 9D).

Late-stage differentiation of the ELPP-coated titanium surfaces as indicated by osteocalcin levels, presented with a more consistent pattern to previous results.[30,31] For all of the ELPP-coated titanium groups, there was an increasing level of osteocalcin that peaked at 21 days except for Ti-pRGD and Ti-pRGD-SNa15 (Figure 10). On the other hand, all of the ELPP-coated titanium surfaces resulted in lower or insignificantly different OCN levels at both 14 and 21 days compared to the negative control group (Ti-cleaned) (Figure 10). Thus, modifying a cleaned titanium surface with bioactive peptide-polymers appeared to not influence or negatively influence the differentiation of pre-

osteoblasts (Figures 9 and 10). Furthermore, coating titanium surfaces with both bioactive peptide-polymers in a 1:1 molar ratio compared to a single polymer with both peptides does not appear influence the differentiation of osteoblasts. These titanium surfaces with both bioactive peptide-polymers do not differ significantly in terms of differentiation compared to titanium surfaces with only one of the bioactive elastin-like peptide-polymers.

RGD

We can only speculate as to the reason for our co-immobilized elastin-like peptide polymer coated titanium surfaces to fail in significantly improving the rate or quality of cellular adhesion, spreading, proliferation, or differentiation. In terms of limitations of the co-immobilized elastin-like polymers with RGD, there may be an insufficient exposure of the RGD motif for cellular adhesion, or the RGD motif and associated protein adsorption may actually change the intracellular signaling and associated differentiation. As discussed previously in the contact angle section, titanium surfaces with elastin-like polymers conform to hide hydrophobic components. Titanium with pRGD has almost the same final contact angle as titanium coated with pRef (Figure 5), so the RGD motif either does not influence the wettability of the modified surface or the RGD is hidden from the water and only presents the hydrophilic part of the elastin-like polymer. The former is probably true because we found improved cell adhesion seen with Ti-pRGD compared to the Ti-pRef (Figure 7). Otherwise, if the later were true, without having an exposed bioactive peptide motif, there would not be improved cellular adhesion and subsequent differentiation. As described earlier, other researchers are

evaluating silanization of bioactive peptides with a short peptide instead of an elastin-like polymer.[36] This simplified short peptide may be a beneficial technique for coating bioactive peptides to titanium because they may prohibit the hiding of bioactive peptides via conformational changes and may promotes their bioactivity.

Another possible explanation for the reduced effectiveness for co-immobilized ELPP-coated titanium surfaces to improve cellular spreading and differentiation is the limit of the RGD peptide itself. The RGD motif is a vital domain in the binding of ECM or cells to integrins. On the other hand, there are adjacent domains that act synergistically in adhesion proteins like fibronectin or vitronectin to strengthen the binding and associated intracellular signaling and subsequent differentiation.[8,38,39] Previous research has noted that a shortened fibronectin sequence to GRGDSP resulted in a 1000 fold decrease in fibronectin-receptor binding affinity than the natural fibronectin peptide alone.[8,39] This could help explain why Ti-pRGD-SNa15 and Ti-1:1 pRGD to SNa15 did not display improved cellular adhesion, spreading, or differentiation compared to the titanium surfaces with a pRef or pSNa15 alone (Figures 6, 7, 9, and 10).

Protein adsorption is an additional consideration with the titanium surface coated with pRGD or pRGD-SNa15. While some research support the theory that adhesive protein adsorption to titanium surfaces improves osseointegration,[35,38,40] there are others that have noted decreased titanium surface mineralization upon surface treatment with sub-clinical adhesive proteins concentrations.[41] Previous research has also noted that protein adsorption is greatest on hydrophobic surfaces and least on hydrophilic surfaces. Thus, hydrophobic surfaces may hinder osseointegration by promoting protein adsorption and decreasing mineralization.[42] The later theory is consistent with our results because

the titanium surfaces with pRGD and pRGD-SNa15 showed increased hydrophobicity and both presented with lower OCN levels at day 21 (Figure 10). Hydrophilicity/hydrophobicity does not account for all mineralization results (OCN levels) as other surfaces with relative hydrophobicity still demonstrated a relatively high level of mineralization at 21 days (i.e. Ti-cleaned, Ti-pRef) (Figures 5 and 10).

The binding affinity of pRGD to pre-osteoblasts may also influence the late-stage differentiation. Titanium coated with pRGD was not only hydrophobic but also demonstrated greater focal adhesion points indicative of cellular adhesion than all other groups. Other studies have noted that when titanium surfaces are coated with RGDs there is greater cellular adhesion and spreading but diminished differentiation. Tosatti et al.[43] reduced protein adsorption and subsequent osteoblast adhesion onto titanium with a coating of poly(ethylene glycol) (PEG), but showed cellular adhesion was restored with adding RGD motifs to the PEG coating. Osteocalcin levels were found to be inversely proportional to RGD density.[43] The role of cellular adhesion and protein adsorption appears to be an important aspect in osteoblastic differentiation. Future research should aim to distinguish what levels are optimal for cellular adhesion, while also promoting osteoblastic differentiation.

SNa15

The statherin-derived sequence (SNa15) has been shown in our research to increase the hydrophilicity of the surface, but not significantly influence osteoblastic adherence or differentiation compared to controls or other ELPP-coated titanium surfaces. There is a similarity of Ti-pSNa15 to Ti-1:1 pRGD to SNa15 with contact

angle, which may be due to conformational changes of the ELPP to hide pRGD and only display SNa15. This makes sense since these two groups acted similar with respect to adhesion, proliferation, and differentiation (Figures 5-10). Unpublished research has noted that a similar ELPP-coated titanium surface with pSNa15 (denoted eTi_HSS) has produced an improved calcium phosphate mineralization layer compared to a titanium surface that was etched or had a reference ELPP.[25] Thus, a titanium surface with pSNa15 may improve the mineralization of the surface but other research has shown that different conformations or ratios of the polymer to peptide may further improve mineralization. Prieto et al.[23] found best calcium phosphate nucleation results with a triblock structure of ELPs with SNa15. The homorecombinamer surface had too many statherin domains, while diblock recombinamer surfaces had too few statherin domains for calcium phosphate nucleation and growth[23] Our study used a homorecombinamer form of the ELP-SNA15, which demonstrated minimal, if any, calcium phosphate nucleation in the study by Prieto et al.[23] and could explain why our pSNa15 titanium surface did not induce significantly greater osteoblastic differentiation (Figure 10).

CONCLUSIONS

Dental implants have become an important option for restoring function, esthetics, and phonetics for patients with edentulous sites. Dental implants are very successful but require a relatively long period of healing before they can be fully loaded and restored. Our research investigated the benefits of covalently coating titanium with biomimetic peptides polymers in terms of *in vitro* osseointegration outcomes. The biomimetic peptide-polymers that we studied are derived from cell-binding proteins (RGD) or a

mineral-binding protein (SNa15) aimed to improve pre-osteoblastic adhesion, proliferation, and differentation.

Previous research has noted the benefits of these biomimetic peptides in terms of cell adhesion, proliferation, and differentiation but few investigators have investigated the osteoblastic response to both biomimetic peptide polymers co-immobilized on the same titanium surface. Furthermore, no other research, to our knowledge, has compared the osteoblastic response between titanium surfaces coated with elastin-like polymers containing both biomimetic peptides (Ti-pRGD-SNa15) to titanium coated with both biomimetic peptides but each being bound on separate elastin-like polymers (Ti-1:1 pRGD to pSNa15).

Our results indicate that titanium coated with an elastin-like polymer with RGD showed the greatest level of cellular adhesion based upon the number of focal adhesion points compared to all other groups. Other ELPP-coated titanium samples, even those with co-immobilized with RGD and SNa15 demonstrated similar or inferior cellular adhesion or spreading compared to controls. All of the ELPP-coated titanium surfaces were not significantly different from each other in terms of proliferation and differentiation. One interesting finding was the association noted between hydrophobicity and late-stage differentiation. Although it did not account for all variability, greater hydrophobicity as seen with Ti-pRGD and Ti-pRGD-SNa15 related to an abnormal late-stage differentiation pattern.

In summary, dental implant surfaces coated with biomimetic peptides are an exciting avenue for future research. Our results indicate that co-immobilization of integrin-binding and statherin-derived biomimetic peptide polymers are not supported at

this time. Future research is needed to optimize this coating process to improve osseointegration-related outcomes. As discussed previously, coating titanium with short peptides or utilizing a triple-block structure for presenting biomimetic peptides may provide a more robust osteoblastic response needed for accelerating dental implant osseointegration.

REFERENCES

1. Esposito M, Grusovin M, Willings M, Coulthard P, Worthington H. The effectiveness of immediate, early, and conventional loading of dental implants: A cochrane systematic review of randomized controlled clinical trials. *The International journal of oral maxillofacial implants*. 2007;22(6):893-904.
2. Brunski JB, Moccia AF, Pollack SR, Korostoff E, Trachtenberg DI. The influence of functional use of endosseous dental implants on the tissue-implant interface. I. histological aspects. *J Dent Res*. 1979;58(10):1953-1969.
3. Aparicio C, Rangert B, Sennerby L. Immediate/early loading of dental implants: A report from the sociedad española de implantes world congress consensus meeting in barcelona, spain, 2002. *Clin Implant Dent Relat Res*. 2003;5(1):57-60.
4. Weber H, Morton D, Gallucci G, Roccuzzo M, Cordaro L, Grutter L. Consensus statements and recommended clinical procedures regarding loading protocols. *The International journal of oral maxillofacial implants*. 2009;24 Suppl:180-183.
5. Fernandez E, Gil FJ, Aparicio C, et al. Materials in dental implantology. In: Natali A, ed. *Dental biomechanics.* London: Taylor and Francis; 2003:69-89.
6. Cooper LF. Biologic determinants of bone formation for osseointegration: Clues for future clinical improvements. *J Prosthet Dent*. 1998;80(4):439-449.
7. Decker J, Lee J, Cortella C, et al. Evaluation of implants coated with recombinant human bone morphogenetic protein-2 and vacuum-dried using the critical-size supraalveolar peri-implant defect model in dogs. *J Periodontol*. 2010;81(12):1839-1849.
8. Ruoslahti E. RGD and other recognition sequences for integrins. *Annu Rev Cell Dev Biol*. 1996;12:697-715.
9. Chen K, Chen X. Integrin targeted delivery of chemotherapeutics. *Theranostics*. 2011;1:189-200.
10. Behravesh E, Zygourakis K, Mikos AG. Adhesion and migration of marrow-derived osteoblasts on injectable in situ crosslinkable poly(propylene fumarate-co-ethylene glycol)-based hydrogels with a covalently linked RGDS peptide. *J Biomed Mater Res A*. 2003;65(2):260-270.
11. Wang X, Heath D, Cooper S. Endothelial cell adhesion and proliferation to PEGylated polymers with covalently linked RGD peptides. *Journal of biomedical materials research.Part A*. 2012;100(3):794-801.
12. Hwang DS, Waite JH, Tirrell M. Promotion of osteoblast proliferation on complex coacervation-based hyaluronic acid - recombinant mussel adhesive protein coatings on titanium. *Biomaterials*. 2009.
13. Ndao M, Ash JT, Breen NF, Goobes G, Stayton PS, Drobny GP. A (13)C{(31)P} REDOR NMR investigation of the role of glutamic acid residues in statherin-hydroxyapatite recognition. *Langmuir*. 2009;25(20):12136-12143.
14. Raj PA, Johnsson M, Levine MJ, Nancollas GH. Salivary statherin. dependence on sequence, charge, hydrogen bonding potency, and helical conformation for adsorption to hydroxyapatite and inhibition of mineralization. *J Biol Chem*. 1992;267(9):5968-5976.
15. Gilbert M, Shaw WJ, Long JR, et al. Chimeric peptides of statherin and osteopontin that bind hydroxyapatite and mediate cell adhesion. *J Biol Chem*. 2000;275(21):16213-16218.

16. Jensen E, Aparicio C, Nedrelow D, et al. Cell response on titanium covalently-coated with multifunctional recombinant biopolymers. *J Dent Res*. 2010;89 (spec iss B); abstract #3573.
17. Werner M, Berguig G, Salvagni E, et al. Novel biomimetic ti surfaces functionalized with genetically-engineered protein-based polymers. *Book of Abstracts. 8th World Biomaterials Congress.* 2008.
18. van Eldijk M, McGann C, Kiick K, van Hest JCM. Elastomeric polypeptides. *Top Curr Chem*. 2012;310:71-116.
19. Girotti A, Reguera J, Rodrguez-Cabello J, Arias F, Alonso M, Matestera A. Design and bioproduction of a recombinant multi(bio)functional elastin-like protein polymer containing cell adhesion sequences for tissue engineering purposes. *Journal of Materials Science: Materials in Medicine*. 2004;15(4):479-484.
20. Nicol A, Gowda DC, Urry DW. Cell adhesion and growth on synthetic elastomeric matrices containing arg-gly-asp-ser-3. *J Biomed Mater Res*. 1992;26(3):393-413.
21. Urry D, Parker T, Reid M, Gowda DC. Biocompatibility of the bioelastic materials, poly(GVGVP) and its γ -irradiation cross-linked matrix: Summary of generic biological test results *J Bioact Compat Polym*. 1991;6:263-282.
22. Di Zio K, Tirrell D. Mechanical properties of artificial protein matrices engineered for control of cell and tissue behavior. *Macromolecules*. 2003;36:1553-1558.
23. Prieto S, Shkilnyy A, Rumplasch C, et al. Biomimetic calcium phosphate mineralization with multifunctional elastin-like recombinamers. *Biomacromolecules*. 2011;12(5):1480-1486.
24. Urry D, Woods T, Hayes L. X, J., et al. Elastic protein-based biomaterials: Elements of basic science, controlled release and biocompatibility. In: Wise D, Hasirci V, Yaszemski M, Altobelli D, Lewandrowski K, Trantolo D, eds. *Biomaterials handbook - advanced applications of basic sciences and bioengineering.* New York, NY: Marcel Dekker; 2003.
25. Li Y, Rodriguez-Cabello C, Aparicio C. Biomimetically-mineralized hybrid coatings on nano-rough titanium functionalized with statherin-inspired recombinant biopolymers. *9th World Biomaterials Congress*. 2012.
26. Kapuscinski J. DAPI: A DNA-specific fluorescent probe. *Biotechnic histochemistry*. 1995;70(5):220-233.
27. Chazotte B. Labeling cytoskeletal F-actin with rhodamine phalloidin or fluorescein phalloidin for imaging. *Cold Spring Harbor protocols*. 2010;2010(5):pdb.prot4947-pdb.prot4947.
28. Xu W, Baribault H, Adamson ED. Vinculin knockout results in heart and brain defects during embryonic development. *Development*. 1998;125(2):327-337.
29. Nanci A. *Ten cate's oral histology: Development, structure, and function.* 6th ed. ed. St. Louis, MO: Mosby; 2003.
30. Owen TA, Aronow M, Shalhoub V, et al. Progressive development of the rat osteoblast phenotype in vitro: Reciprocal relationships in expression of genes associated with osteoblast proliferation and differentiation during formation of the bone extracellular matrix. *J Cell Physiol*. 1990;143(3):420-430.
31. Lian JB, Stein GS. Concepts of osteoblast growth and differentiation: Basis for modulation of bone cell development and tissue formation. *Critical reviews in oral biology and medicine*. 1992;3(3):269-305.

32. Lian JB, Gundberg CM. Osteocalcin. biochemical considerations and clinical applications. *Clin Orthop*. 1988(226):267-291.
33. Schwarz F, Wieland M, Schwartz Z, et al. Potential of chemically modified hydrophilic surface characteristics to support tissue integration of titanium dental implants. *Journal of biomedical materials research.Part B, Applied biomaterials*. 2009;88(2):544-557.
34. Urry D, Woods C, Hayes L, et al. Elastic protein-based biomaterials: Elements of basic science, controlled release and biocompatibility. In: Yaszemski M, Trantolo D., Lewandrowski K, Hasirci V., Altobelli D, Wise D., eds. *Tissue engineering and novel delivery systems.* CRC Press; 2003:31-54.
35. Garcia AJ. Get a grip: Integrins in cell-biomaterial interactions. *Biomaterials*. 2005;26(36):7525-7529.
36. Sevilla P, Godoy M, Salvagni E, Rodriquez D, Gil F. Biofunctionalization of titanium surfaces for osseintegration process improvement. *J Phys: Conf Ser*. 2010;252:012009.
37. Chen X, Sevilla P, Aparicio C. Biofunctionalization of ti surfaces by covelant co-immobilization of the synergistic RGD and PHSRN oligopeptides. *9th World Biomaterials Congress*. 2012.
38. Hennessy K, Clem W, Phipps M, Sawyer A, Shaikh F, Bellis S. The effect of RGD peptides on osseointegration of hydroxyapatite biomaterials. *Biomaterials*. 2008;29(21):3075-3083.
39. Hautanen A, Gailit J, Mann DM, Ruoslahti E. Effects of modifications of the RGD sequence and its context on recognition by the fibronectin receptor. *J Biol Chem*. 1989;264(3):1437-1442.
40. Bagambisa FB, Kappert HF, Schilli W. Cellular and molecular biological events at the implant interface. *Journal of cranio-maxillo-facial surgery*. 1994;22(1):12-17.
41. do Serro AP, Fernandes AC, de Jesus Vieira Saramago B. Calcium phosphate deposition on titanium surfaces in the presence of fibronectin. *J Biomed Mater Res*. 2000;49(3):345-352.
42. Tugulu S, Lwe K, Scharnweber D, Schlottig F. Preparation of superhydrophilic microrough titanium implant surfaces by alkali treatment. *Journal of materials science: Materials in medicine*. 2010;21(10):2751-2763.
43. Tosatti S, Schwartz Z, Campbell C, et al. RGD-containing peptide GCRGYGRGDSPG reduces enhancement of osteoblast differentiation by poly(L-lysine)-graft-poly(ethylene glycol)-coated titanium surfaces. *Journal of biomedical materials research.Part A*. 2004;68(3):458-472.